ChemComm

RSC Publishing

COMMUNICATION

View Article Online
View Journal | View Issue

# A two-dimensional zeolitic imidazolate framework with a cushion-shaped cavity for $CO_2$ adsorption†

Cite this: *Chem. Commun.*, 2013, **49**, 9500

Received 9th June 2013,
Accepted 16th August 2013

DOI: 10.1039/c3cc44342f

www.rsc.org/chemcomm

Rizhi Chen,[ab] Jianfeng Yao,[a] Qinfen Gu,[c] Stef Smeets,[d] Christian Baerlocher,[d] Haoxue Gu,[b] Dunru Zhu,[b] William Morris,[e] Omar M. Yaghi[f] and Huanting Wang*[a]



**A new two-dimensional zeolitic imidazolate framework (named as ZIF-L) was synthesized in zinc salt and 2-methylimidazole (Hmim) aqueous solution at room temperature. ZIF-L ($Zn(mim)_2{\cdot}(Hmim)_{1/2}{\cdot}(H_2O)_{3/2}$ or $C_{10}H_{16}N_5O_{3/2}Zn$) has unique cushion-shaped cavities and leaf-like crystal morphology, and exhibits excellent $CO_2$ adsorption properties.**

Zeolitic imidazolate frameworks (ZIFs) are highly ordered porous solids, which consist of inorganic metal ions in tetrahedral environments bridged by imidazolate ligands.[1–3] The topological and porous structure of ZIFs can be designed and controlled by using various imidazolate units.[2,3] A large variety of ZIFs have been reported, and they are typically synthesized in organic solvents such as *N*,*N*-dimethylformamide (DMF), diethylformamide or methanol.[1,2,4,5] More recently, ZIF-8 and ZIF-67 have also been synthesized in aqueous solutions.[6–8] It has been shown that synthesis conditions have a significant effect on the ZIF crystallization process and thus crystal morphology, size, and topology.[8,9] For example, the crystal size of ZIF-8 could be adjusted by varying the concentration of 2-methylimidazole (Hmim) and zinc ions in the aqueous based reaction.[7] ZIF-8 crystals with different morphologies including hexagonal plates and rhombic dodecahedrons were synthesized by addition of an organic polymer[10] or cetyltrimethylammonium bromide,[11] respectively. However, to date no new topologies of Hmim and a zinc source have been reported.

ZIFs have been widely studied for their potential use as adsorbents and membranes for carbon dioxide capture as part of global efforts in reducing the sharply rising level of atmospheric carbon dioxide resulting from anthropogenic emissions.[12–15] Strategies developed for designing high-efficiency $CO_2$ selective ZIFs or MOFs thus far include the construction of large cages, tailoring of pore apertures and framework chemistry.[16] For instance, a large volume of $CO_2$ can be effectively retained in the colossal cages of ZIF-95 and ZIF-100 while the other gases pass through without hindrance due to the combined effects of the slit width of the pore apertures being similar in size to linear and centrosymmetric carbon dioxide and the strong quadrupolar interactions of carbon with nitrogen atoms present in the ligands.[1] Sod-ZMOF was shown to have superior $CO_2$ adsorption capacity compared to ZIF-8 though ZIF-8 has a much higher surface area; this was likely because ZIF-8 adsorbed $CO_2$ through van der Waals forces only whereas ZMOF materials with cations inside the pores could interact with $CO_2$.[17]

Herein we report a new two-dimensional zeolitic imidazolate framework (ZIF) with a cushion-shaped cavity between layers with a dimension of 9.4 Å × 7.0 Å × 5.3 Å and a leaf-shaped morphology (named as ZIF-L). This cushion-shaped cavity is unique, and well suited to accommodate $CO_2$ molecules. ZIF-L is comprised of the identical building blocks of ZIF-8 Hmim and zinc nitrate but possesses a different topology.

ZIF-L was synthesized from zinc nitrate hexahydrate and Hmim in deionized water at room temperature, and its key synthesis parameter was the ratio of Hmim/zinc ion molar ratio (*e.g.*, 8). The yield of ZIF-L was over 80% on the basis of the amount of zinc nitrate used. The composition of ZIF-L prior to activation was determined to be $Zn(mim)_2{\cdot}(Hmim)_{1/2}{\cdot}(H_2O)_{3/2}$ ($C_{10}H_{16}N_5O_{3/2}Zn$) by elemental analysis, which was confirmed by TG analysis (Fig. S1, ESI†). The single crystals were not suitable for single crystal determination due to their small sizes; however, we successfully determined the structure of ZIF-L from synchrotron powder X-ray diffraction data (Table S1, ESI†). As shown in Fig. 1, the Rietveld refinement shows good agreement with the experimental X-ray diffraction results with agreement factors of $R_p$ = 8.02%, $R_{wp}$ = 7.55%, and GOF = 1.538, which validate our structure solution. ZIF-L crystallizes in the orthorhombic system, space group *Cmce*, with cell parameters of $a$ = 24.1191(5) Å, $b$ = 17.0604(3) Å and $c$ = 19.7398(4) Å. There are two crystallographically different Zn(II) ions, four Hmim ligands and one "free" Hmim molecule (Hmim-5)

[a] *Department of Chemical Engineering, Monash University, Clayton, Victoria 3800, Australia. E-mail: huanting.wang@monash.edu; Fax: +61 3 9905 5686; Tel: +61 3 9905 3449*
[b] *State Key Laboratory of Materials-Oriented Chemical Engineering, Nanjing University of Technology, Nanjing 210009, P. R. China*
[c] *Australian Synchrotron, Clayton, VIC 3168, Australia*
[d] *ETH Zurich, Laboratory of Crystallography, CH-8093 Zurich, Switzerland*
[e] *Department of Chemistry, Northwestern University, Evanston, IL 60208, USA*
[f] *Department of Chemistry, University of California-Berkeley, and Molecular Foundry, Lawrence Berkeley National Laboratory, Berkeley, CA 94720, USA*

† Electronic supplementary information (ESI) available: Synthesis and characterization, $CO_2$ and $CH_4$ adsorption isotherms, three cycles of $CO_2$ adsorption and desorption isotherms, structure determination and stability; Tables S1 and S2 and Fig. S1–S11. See DOI: 10.1039/c3cc44342f

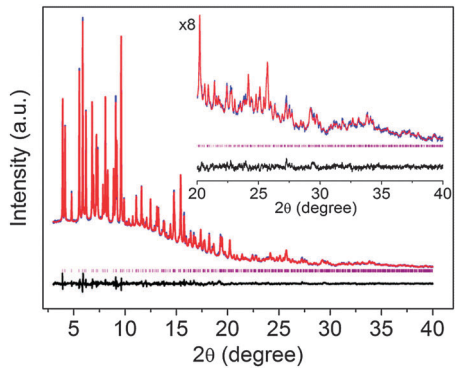


**Fig. 1** Rietveld refinement profile for the ZIF-L sample showing observed (blue line), calculated (red line), and difference (black line) plots. The positions of Bragg reflections (tick marks) are shown for ZIF-L. The data were collected at a wavelength of 0.8237 Å at room temperature.

in the asymmetric unit (Fig. 2). Each Zn atom adopts a regular [$ZnN_4$] tetrahedral geometry where Zn1 is coordinated by four $\mu_2$-bridging N atoms (N16, N16, N26 and N26) of two imidazole units while Zn2 is coordinated by N atoms (N15, N25, and N35) of three imidazole units and a monodentate one containing N45. The Hmim-1 ligand with N15/N16 as a $\mu_2$-bridge links Zn1 and Zn2 ions with a distance of 6.01 Å while Hmim-2 with N25/N26 connects Zn1 and Zn2 ions with a distance of 5.96 Å (Fig. 2). In addition, Hmim-3 forms a $\mu_2$-bridge between 2 Zn2 ions with a distance of 6.07 Å.

Six $\mu_2$-bridging Hmim ligands bind two Zn1 ions in opposite position and four Zn2 ions to form a large hexagon, while four $\mu_2$-bridging Hmim ligands bind two Zn1 and two Zn2 ions to produce a smaller parallelogram. These hexagons and parallelograms are interconnected to create a 2D layer network along the *ab* plane and these layers are then stacked along the *c* direction (Fig. 3a). These layers are part of the sodalite (SOD) topology found in the 3D structure of ZIF-8 (Fig. 3b).[4] The 2D network is further stabilized by the interdigitating interactions with the help of the terminal Hmim-4 ligands containing N46 atoms and the "free" Hmim-5 between the layers (Fig. 4). Hmim-5 is hydrogen bonded to the N46 atoms of Hmim-4 and its ring lies parallel to the ring of Hmim-3, potentially forming a weak interaction with the neighbouring layer.

ZIF-L does have one large zero-dimensional pore or cavity with dimensions of 9.4 Å × 7.0 Å × 5.3 Å. This cushion-shaped cavity is shown in Fig. 5a. In principle, such a unique cavity is well suited to accommodate $CO_2$ molecules as determined by a Rietveld refinement. ZIF-L structure does not change after $CO_2$ adsorption, as confirmed

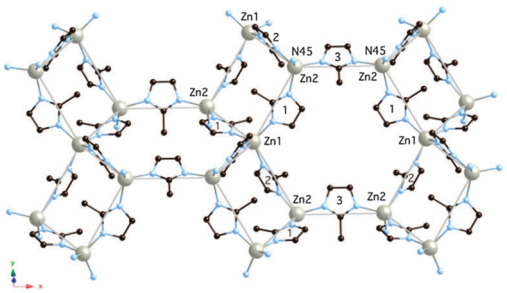


**Fig. 2** The 2D layer in ZIF-L showing the linking Hmim molecules (numbers 1 to 3) and the N atom (N45) of the monodentated Hmim-4. C: black; N: light blue; Zn: gray. Hydrogen atoms are omitted for clarity.

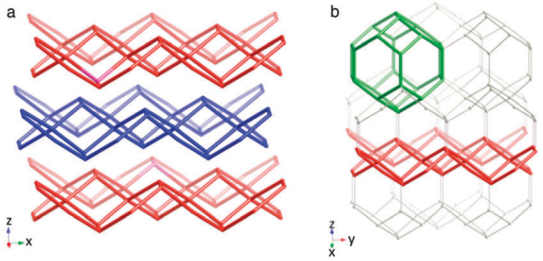


**Fig. 3** (a) Two-dimensional layer structure of ZIF-L along *z*, (b) sod topology of ZIF-8. Relationship between ZIF-8 and ZIF-L: ZIF-8 framework (grey color) with a sodalite cage highlighted in green and the layer corresponding to ZIF-L in red. Only the network of the Zn atoms is shown.

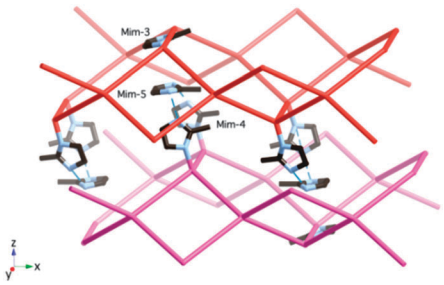


**Fig. 4** The interdigitating interactions between neighboring 2D networks in ZIF-L. The groups formed by Hmim-4 and Hmim-5 molecules point into the "cups" of the opposing layer. For clarity not all Hmim molecules are shown.

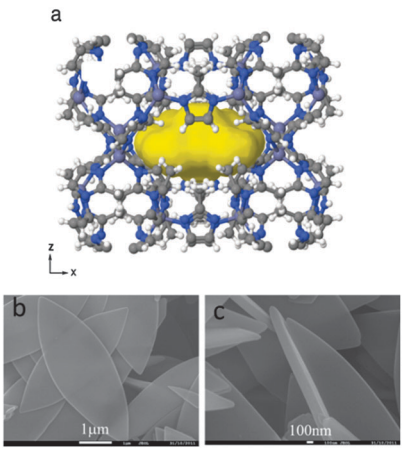


**Fig. 5** (a) The structure of ZIF-L viewed along *y* with an isosurface showing the location and approximate shape of the cavity (yellow). This isosurface was calculated using the program Jmol (Jmol: an open-source Java viewer for chemical structures in 3D. http://www.jmol.org/). (b, c) SEM images of typical ZIF-L crystals: (b) top view image showing leaf-like shape and (c) side view image showing the crystal thickness.

by its XRD pattern (Fig. S2, ESI†). SEM images of typical ZIF-L crystals are shown in Fig. 5b and c. These ZIF-L crystals exhibit a unique leaf-like shape with a size of about 5 μm × 2 μm and a thickness of about 150 nm. ZIF-L crystals with two-dimensional leaf-like morphology may be very useful as building blocks for the fabrication of thin ZIF-L membranes and nanocomposite membranes for separation applications.[18,19]

Like ZIF-8, ZIF-L does not have a channel system, so the $CO_2$ sorption must also occur *via* a gate opening mechanism as proposed for ZIF-8 and other ZIFs and MOFs (Fig. S3, ESI†).[20–23] Such a cavity

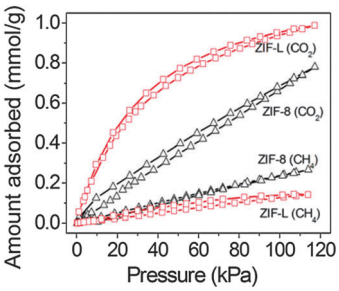


**Fig. 6** $CO_2$ and $CH_4$ adsorption–desorption isotherms of ZIF-L and ZIF-8 measured at 298 K.

is much more flexible than the tetrahedral structure of ZIFs because it is located between the 2D layers that are weakly connected by the terminal Hmim-4 and "free" Hmim-5. The superior $CO_2$ adsorption selectivity of ZIF-L was confirmed by adsorption experiments. The $CO_2$ and $CH_4$ adsorption–desorption curves of ZIF-L at room temperature are shown in Fig. 6. ZIF-L crystals adsorb $CO_2$ preferentially over $CH_4$, and exhibit superior $CO_2$ adsorption capacity (0.94 mmol $g^{-1}$) and $CO_2/CH_4$ adsorption selectivity (7.2) as compared with other ZIFs with large cages (Table S2, ESI†).

This result should be attributed to unique cushion-shaped cavities and strong interactions between $CO_2$ molecules and Hmim molecules. The shortest distances from the O atoms of the $CO_2$ molecules to H atoms of methylimidazole molecules are those to H43 and H52 of the Hmim-4 and Hmim-5 molecules. The Hmim-4 molecule is only connected to one zinc atom in ZIF-L structure and the Hmim-5 molecule is totally "free". Contrary to what one might expect, there is no direct contact with the N atoms of any Hmim molecules in ZIF-L. It is noted that the ZIF-L sample has a micropore volume of 0.066 $cm^3$ $g^{-1}$, a BET surface area of 161 $m^2$ $g^{-1}$ and a Langmuir surface area of 212 $m^2$ $g^{-1}$. The surface area and micropore volume of ZIF-L are lower than those of ZIF-8 (Fig. S3, ESI†).[4] This is because ZIF-L has smaller pore size and higher density (density of metal atoms per unit volume) than ZIF-8. As summarized in Table S2 (ESI†), ZIF-L shows higher $CO_2$ adsorption capacity and $CO_2/CH_4$ adsorption selectivity than ZIF-8, ZIF-95, and ZIF-100 although ZIF-L has much lower surface area than other ZIFs; but ZIF-L has lower $CO_2$ adsorption capacity and $CO_2/CH_4$ adsorption selectivity than some MOFs such as NOTT-300 (Table S2, ESI†). In order to evaluate the reversibility of $CO_2$ adsorption on ZIF-L, the $CO_2$ adsorption–desorption process was repeated at 298 K for three cycles. The curves for the 2nd and the 3rd cycle are very similar to that for the 1st cycle of the $CO_2$ adsorption–desorption process, suggesting that $CO_2$ can be easily adsorbed and desorbed from ZIF-L (Fig. S4, ESI†). The preferential adsorption of $CO_2$ over other gases makes ZIF-L crystals highly attractive for $CO_2$ separation and capture in many industrial processes.

We also studied the thermal stability of ZIF-L (Fig. S5–S10, ESI†), and the results showed that ZIF-L is stable at 150 °C in air. To study the structural stability of ZIF-L, X-ray diffraction experiments were performed at high pressures by Synchrotron measurements (Fig. S11, ESI†). Except for the peak broadening, no drastic structural changes of the diffraction pattern were observed up to 6.3 GPa. Due to limited peak intensities, detailed structure investigation was not possible from the data. After the pressure was released, the XRD peaks somewhat shifted to lower angles compared with the XRD pattern collected before the high-pressure study (Fig. S11, ESI†). A slightly larger unit cell was observed in the recovered sample likely because the pressure medium was pressed into ZIF-L structure pores. Therefore, this result indicates that ZIF-L exhibits excellent structural stability at high pressures.

A new two-dimensional ZIF-L structure was synthesized at ambient temperature by controlling the Hmim/Zn ratio in an aqueous solution. Leaf-shaped ZIF-L crystals have cushion-shaped cavities that ideally accommodate $CO_2$ molecules; they exhibit higher $CO_2$ adsorption capacity and selectivity than the ZIFs with large cages such as ZIF-8, ZIF-95 and ZIF-100 under ambient conditions. This result indicates that tailoring the cavity shape can be an effective way to design ZIFs with enhanced adsorption properties. Owing to its excellent $CO_2$ adsorption properties and high pressure stability, ZIF-L shows great potential for use as an adsorbent and membrane material for $CO_2$ adsorption and separation applications.

H.W. thanks the ARC for a Future Fellowship (FT100100192). J.Y. thanks Monash University for a Monash Fellowship. This project was in part supported by NKSTPC (2011BAE07B05), NNSFC (20990222, 21106061, and 21171093), and NSF of Jiangsu Province (BK2010549, BK2009021). S.S. thanks the Swiss National Science Foundation for support. Part of experimental work was conducted at the Australian Synchrotron.

## Notes and references

1 R. Banerjee, A. Phan, B. Wang, C. Knobler, H. Furukawa, M. O'Keeffe and O. M. Yaghi, *Science*, 2008, **319**, 939–943.
2 R. Banerjee, H. Furukawa, D. Britt, C. Knobler, M. O'Keeffe and O. M. Yaghi, *J. Am. Chem. Soc.*, 2009, **131**, 3875–3877.
3 A. S. Huang, H. Bux, F. Steinbach and J. Caro, *Angew. Chem., Int. Ed.*, 2010, **49**, 4958–4961.
4 K. S. Park, Z. Ni, A. P. Cote, J. Y. Choi, R. D. Huang, F. J. Uribe-Romo, H. K. Chae, M. O'Keeffe and O. M. Yaghi, *Proc. Natl. Acad. Sci. U. S. A.*, 2006, **103**, 10186–10191.
5 X. C. Huang, Y. Y. Lin, J. P. Zhang and X. M. Chen, *Angew. Chem., Int. Ed.*, 2006, **45**, 1557–1559.
6 Y. C. Pan, Y. Y. Liu, G. F. Zeng, L. Zhao and Z. P. Lai, *Chem. Commun.*, 2011, **47**, 2071–2073.
7 K. Kida, M. Okita, K. Fujita, S. Tanaka and Y. Miyake, *CrystEngComm*, 2013, **15**, 1794–1801.
8 J. F. Yao, M. He, K. Wang, R. Z. Chen, Z. X. Zhong and H. T. Wang, *CrystEngComm*, 2013, **15**, 3601–3606, DOI: 10.1039/C3CE27093A.
9 Q. Shi, Z. F. Chen, Z. W. Song, J. P. Li and J. X. Dong, *Angew. Chem., Int. Ed.*, 2011, **50**, 672–675.
10 S. K. Nune, P. K. Thallapally, A. Dohnalkova, C. M. Wang, J. Liu and G. J. Exarhos, *Chem. Commun.*, 2010, **46**, 4878–4880.
11 Y. C. Pan, D. Heryadi, F. Zhou, L. Zhao, G. Lestari, H. B. Su and Z. P. Lai, *CrystEngComm*, 2011, **13**, 6937–6940.
12 J. R. Li, J. Sculley and H. C. Zhou, *Chem. Rev.*, 2012, **112**, 869–932.
13 K. Sumida, D. L. Rogow, J. A. Mason, T. M. McDonald, E. D. Bloch, Z. R. Herm, T. H. Bae and J. R. Long, *Chem. Rev.*, 2012, **112**, 724–781.
14 Y. S. Bae and R. Q. Snurr, *Angew. Chem., Int. Ed.*, 2011, **50**, 11586–11596.
15 A. Phan, C. J. Doonan, F. J. Uribe-Romo, C. B. Knobler, M. O'Keeffe and O. M. Yaghi, *Acc. Chem. Res.*, 2010, **43**, 58–67.
16 J. R. Li, Y. G. Ma, M. C. McCarthy, J. Sculley, J. M. Yu, H. K. Jeong, P. B. Balbuena and H. C. Zhou, *Coord. Chem. Rev.*, 2011, **255**, 1791–1823.
17 C. Chen, J. Kim, D. A. Yang and W. S. Ahn, *Chem. Eng. J.*, 2011, **168**, 1134–1139.
18 K. Varoon, X. Y. Zhang, B. Elyassi, D. D. Brewer, M. Gettel, S. Kumar, J. A. Lee, S. Maheshwari, A. Mittal, C. Y. Sung, M. Cococcioni, L. F. Francis, A. V. McCormick, K. A. Mkhoyan and M. Tsapatsis, *Science*, 2011, **333**, 72–75.
19 M. A. Snyder and M. Tsapatsis, *Angew. Chem., Int. Ed.*, 2007, **46**, 7560–7573.
20 G. Ferey and C. Serre, *Chem. Soc. Rev.*, 2009, **38**, 1380–1399.
21 D. Fairen-Jimenez, S. A. Moggach, M. T. Wharmby, P. A. Wright, S. Parsons and T. Duren, *J. Am. Chem. Soc.*, 2011, **133**, 8900–8902.
22 S. A. Moggach, T. D. Bennett and A. K. Cheetham, *Angew. Chem., Int. Ed.*, 2009, **48**, 7087–7089.
23 C. Gucuyener, J. van den Bergh, J. Gascon and F. Kapteijn, *J. Am. Chem. Soc.*, 2010, **132**, 17704–17706.



 